35th Annual International Conference of the IEEE EMBS
Osaka, Japan, 3 - 7 July, 2013

Reconstruction of Missing Cells by a Killing Energy Minimizing Nonrigid Image Registration

Ken Y.K. Chan[1] and Justin W.L. Wan[2]

Abstract— **Fluorescent microscopy has been a popular and important tool for studying live cells. One challenge of analyzing cell images obtained from fluorescent microscopy is that cells in fluorescent images frequently disappear and reappear, making cell tracking difficult. In this paper, we present an image registration approach which can reconstruct both the cell appearance and location of the missing cells from the image frames where the cells become invisible. The idea is to perform an image registration on the images before and after a cell disappears. The missing image frames between these two images are given by the intermediate registration results. The formulation is based on the nonrigid particle registration model, which captures soft deformation of the cells. In addition, to obtain natural and more rigid cell movements such as translation and rotation, we propose a new registration technique which is Killing energy minimizing, motivated by the fact that a Killing vector field with zero Killing energy will generate an isometric deformation. We will present reconstruction results of C2C12 cells in fluorescent images to illustrate the effectiveness of our model by different numerical examples.**

I. INTRODUCTION

In fluorescent microscopy [1], cells are tagged with protein markers that will fluorescence when exposed to light of specific wavelengths. The intensity of visible light emitted depends on the environment and in particular, the amount of the fluorophores which are components of the protein markers that cause molecules to be fluorescent. The fluorescent part of a cell (in our experiments, the nucleus) shows a distinct color which makes it easily distinguishable from the background, yielding high contrast images suitable for image analysis.

However, the intensities of the fluorophores may fluctuate over time. When the intensity level is below certain threshold, the cells may not be fluoresced. It has been observed in the literature that cells in fluorescent images frequently "disappear" [2]. Thus a cell may initially appear in an image frame, but then later becomes invisible in the subsequent frames. When the intensities of the fluorophores build up again, the cell may "reappear" in later frames, possibly at a different location. It is not clear if using different fluorophores might prevent the problem.

The frequent disappearance and reappearance of cells pose challenges to tracking cells in fluorescent images. When a cell becomes invisible, it is not known if it will reappear and if it does, when and where it will appear again. When a cell eventually becomes visible, it may be mistakenly considered as a nearby cell from the previous frame, rather than being recognized as the missing cell from a number of frames before. Manually connecting disappeared cells to reappeared cells can be tedious and error prone.

While the issue of frequent cell disappearance is known, it was seldom discussed in the literature. A recent approach [3] addressed the issue by exploiting the temporal information. Specifically, image frames are stacked together to form a 3D image volume [4]. In fluorescent images, cells often appear as bright, convex shaped objects. The path of a cell forms a "tube" in the image volume. The disappearance of a cell creates a gap in the cell tube. A 3D-2D segmentation model was developed which performs 2D segmentation to capture the cells that appear in the image frames and 3D segmentation to locate the missing cells. This technique was later extended to reconstruct cells where cell divisions have taken place [5].

The segmentation approach [3] is able to find the locations, or more precisely, the boundary of the missing cells. However, it does not provide any information inside the cell. The extended approach [5] attempts to estimate the cell appearance by interpolation. It shows some intensity variation inside the cell but hardly any details.

The importance of this research is to address the cell disappearance issue by accurately reconstructing the invisible cells so that cell tracking could be done more reliably. In this paper, we propose the use of image registration method to reconstruct the missing cells. The idea is to reconstruct the location as well as the appearance of the cell on the image frames where it is not visible by registering the images of the cell before and after it disappears. However, simply applying the standard nonrigid registration methods will typically result in unnatural movement and shape of the missing cell. Instead, we propose a novel image registration technique based on minimizing the Killing energy. It is able to reproduce the translation and rotational motions that often occur in cell movements.

II. METHODOLOGY

The goal of the proposed registration technique is to reconstruct both the appearance of the missing cell and its location. The key idea is that connecting the two broken parts of a cell tube can be viewed as an image registration process. More precisely, consider the image right before the cell disappears and another image right after it reappears. We perform an

*This work was supported by the Natural Sciences and Engineering Research Council of Canada.

[1]K. Chan is with the David R. Cheriton School of Computer Science, University of Waterloo, Ontario N2L 3G1, Canada. kyk2chan@uwaterloo.ca

[2]J. Wan is with the David R. Cheriton School of Computer Science, University of Waterloo, Ontario N2L 3G1, Canada. jwlwan@uwaterloo.ca

978-1-4577-0216-7/13/$26.00 ©2013 IEEE

image registration to align these two images. During the registration process parametrized by time t, one cell image (the template), $I_1(\boldsymbol{x})$, evolves to align with the other cell image (the target), $I_2(\boldsymbol{x})$. At the end of the process at time $t = T$, the transformed template $I_1(\boldsymbol{x}-\boldsymbol{r}(\boldsymbol{x},T))$ aligns with the target $I_2(\boldsymbol{x})$, where $\boldsymbol{r}$ denotes the displacement. If we put all the intermediate images, $I_1(\boldsymbol{x}-\boldsymbol{r}(\boldsymbol{x},t))$, $0 \le t \le T$, produced by the registration process together, they will then form a 3D image volume in which a cell tube was formed by the intermediate transformed template images that connects the cells at the two ends.

Our approach is based on the particle nonrigid registration model [6]. Nonrigid registration methods [7] have the advantage of aligning cells of different shapes, which are necessary for live cells. In the particle nonrigid registration approach, the template image is modelled as a set of particles moving towards the target image under an applied force. At any time t, the displacement vector $\boldsymbol{r}(\boldsymbol{x},t)$ is given by the solution of the following minimization problem:

$$\min_{\boldsymbol{r}} \int_\Omega \frac{\alpha}{2}|I_1(\boldsymbol{x}-\boldsymbol{r}(\boldsymbol{x},t))-I_2(\boldsymbol{x})|^2\,d\boldsymbol{x}+\beta\int_\Omega \frac{1}{2}\|\boldsymbol{u}(\boldsymbol{x},t)\|^2\,d\boldsymbol{x}, \tag{1}$$

where α, β are parameters, and $\boldsymbol{u} = d\boldsymbol{r}/dt$ is the velocity. The distance measure in (1) drives the registration process while the kinetic energy regularization term minimizes the motion. The interaction of the two terms move the template to the target with minimal motion.

The particle registration model leads to the following system of partial differential equations:

$$\boldsymbol{b}(\boldsymbol{x},t) = \alpha(I(\boldsymbol{x},t)-I_2(\boldsymbol{x}))\frac{\nabla I(\boldsymbol{x},t)}{\|\nabla I(\boldsymbol{x},t)\|}, \tag{2}$$

$$\frac{\partial \boldsymbol{u}(\boldsymbol{x},t)}{\partial t} = \boldsymbol{b}(\boldsymbol{x},t)-\boldsymbol{u}(\boldsymbol{x},t)\cdot\nabla\boldsymbol{u}(\boldsymbol{x},t), \tag{3}$$

$$\frac{\partial \boldsymbol{r}(\boldsymbol{x},t)}{\partial t} = \boldsymbol{u}(\boldsymbol{x},t)-\boldsymbol{u}(\boldsymbol{x},t)\cdot\nabla\boldsymbol{r}(\boldsymbol{x},t), \tag{4}$$

where $\boldsymbol{b}(\boldsymbol{x},t)$ is the applied body force and $I(\boldsymbol{x},t) = I_1(\boldsymbol{x}-\boldsymbol{r}(\boldsymbol{x},t))$ denotes the deformed template. During the registration process, in each time step, the function $\boldsymbol{b}(\boldsymbol{x},t)$ generates a body force to deform the template towards the target. Then the velocity is updated using the body force. Note that the velocity equation (3) is derived based on the Eulerian framework. Finally, the displacement $\boldsymbol{r}(\boldsymbol{x},t)$ is updated using the velocity by (4).

As shown in Fig. 1 (top), the particle nonrigid registration is able to correctly transform a circle (representing a cell) from one position to another. However, the registration process creates an unnatural motion of the circle from one position to the other. Intuitively, one would expect a simple translation, shown in Fig. 1 (bottom) but instead, the circle shrinks on the left side and expands on the right side, which would not be a desirable reconstruction of the circle between the template and target.

A. Killing energy minimizing image registration

Nonrigid registration models allow objects to deform into different shapes, but it usually does not produce rigid motions

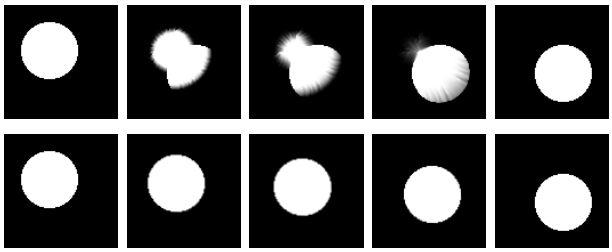

Fig. 1. Registration results of a translated circle given by (top) the particle model, and (bottom) the Killing energy minimizing model.

such as translation and rotation, which are common movements of cells. Motions such as translation and rotation are global where all points on the image move in the same way and at same time. This might not usually happen in standard nonrigid models since their registration process typically is driven by the difference of the template and target. At the region where an object on the template overlap with itself on the target, there will be no difference and hence no motion. As shown in Fig. 1, when a cell is moved to the right, a standard nonrigid registration model would typically shrink the cell towards the overlap region and then expand it to the new position. The final alignment is still valid but the process is not as intuitive, which is important to us for reconstructing the missing cell.

To avoid this undesirable motion, we propose to incorporate Killing[1] energy [8] for the velocity field $\boldsymbol{u}$:

$$E_K(\boldsymbol{u}) \equiv \int \|J_{\boldsymbol{u}}(\boldsymbol{x}) + J_{\boldsymbol{u}}(\boldsymbol{x})^T\|_F^2, \tag{5}$$

into the registration model. Here $J_{\boldsymbol{u}}$ is the Jacobian of the vector field $\boldsymbol{u}$. Vector fields with zero Killing energy are called Killing vector fields (KVFs). One useful and important property of KVFs is that they generate isometric deformations including translation and rotation.

In order to capture the translation and rotation components of the cell movements, after we compute the velocity field $\boldsymbol{u}$ from (3), instead of using it to update $\boldsymbol{r}$, we substitute it by a KVF which is close to $\boldsymbol{u}$. For any KVF $\boldsymbol{v} = (v^1, v^2)$, one can show that it satisfies the following equalities:

$$\frac{\partial v^1}{\partial x} = 0,\ \frac{\partial v^2}{\partial y} = 0,\ \frac{\partial v^1}{\partial y} + \frac{\partial v^2}{\partial x} = 0.$$

In general, however, there may not exist a vector field which is close to $\boldsymbol{u}$ and satisfies all the equalities.

Instead, we look for vector fields that are "as-Killing-as-possible" [9]. More precisely, we find a vector field $\tilde{\boldsymbol{u}}$ such that it minimizes the following energy functional:

$$\min_{\boldsymbol{v}} \frac{1}{4}E_K(\boldsymbol{v}) + \lambda\|\boldsymbol{v}-\boldsymbol{u}\|^2, \tag{6}$$

where λ is a parameter that controls how much Killing is desired. Instead of insisting on a KVF which may not exist, this formulation find a balance between requiring the vector field to be Killing and be close to the given velocity field $\boldsymbol{u}$.

[1]The term "Killing" is named after the mathematician Wilhelm Killing.

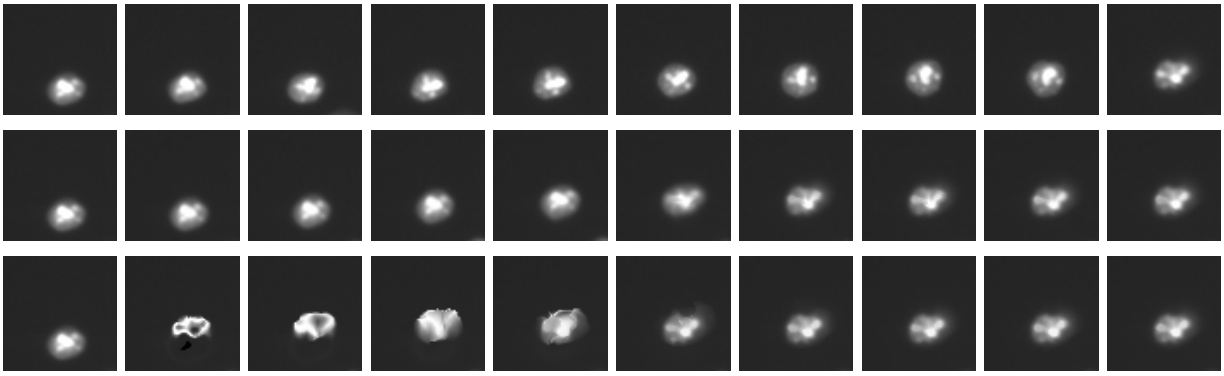

Fig. 2. Reconstruction results of image frames where a cell is removed from a gap of size 8 frames with the left and right images as given. (Top) original cell images, (middle) reconstruction given by the Killing energy minimizing registration, and (bottom) reconstruction given by the particle registration.

A finite difference discretization of (6) yields the following least squares problem:

$$\min \left\| \begin{bmatrix} P \\ \lambda I \end{bmatrix} \begin{bmatrix} v^1 \\ v^2 \end{bmatrix} - \begin{bmatrix} 0 \\ \boldsymbol{u} \end{bmatrix} \right\|^2,$$

where $\boldsymbol{u} = (u^1, u^2)$, I is the identity matrix of size $2n \times 2n$, n is the number of grid points, and P is given by

$$P = \begin{bmatrix} D_x & 0 \\ 0 & D_y \\ D_y & D_x \end{bmatrix}.$$

Here D_x and D_y are the discrete operators corresponding to the partial derivatives w.r.t. x and y, respectively. The least squares problem can be solved by QR factorization.

In the end, we have obtained an as-Killing-as-possible vector field $\tilde{\boldsymbol{u}}$ which will be used instead of $\boldsymbol{u}$ to update the displacement $\boldsymbol{r}$ in (4).

As the registration process progresses, one of cell images (the template) will gradually evolve into the other cell image (the target). Due to the Killing energy model, the modified velocity vector field is close to a KVF, which is now able to reconstruct more natural cell movements such as translation and rotation; see Fig. 1 (bottom).

B. Reconstruction of image frames

The final step is to match the missing image frames with the intermediate transformed templates generated during the particle registration process. In general, these intermediate templates are far more abundant than the original missing frames. Since our model is a flow model in nature, in which the magnitude of the underlying velocity field depends on the difference between the transformed template with the target image during each time step. The magnitude decreases as the transformed template becomes more resemble to the target. Consequently, the naïve approach of matching the missing frames by a liner interpolation performs poorly in general. Denote by $F_{\rm src}$ (resp. $F_{\rm reg}$) the number of missing frames (resp. deformed templates), and by $I_{\rm src}$ (resp. $I_{\rm reg}$) the index of missing frames (resp. templates). We consider two nonlinear index matching rules:

$$I_{\rm reg} = \left\lfloor \frac{F_{\rm reg} - 1}{(F_{\rm src} - 1)^2} (I_{\rm src} - 1)^2 + 1 \right\rfloor, \qquad (7)$$

$$I_{\rm reg} = \left\lfloor 1 - \frac{F_{\rm reg} - 2}{\log(2F_{\rm src} - 3)} \log\left(\frac{2F_{\rm src} - 2}{I_{\rm src} + F_{\rm src} - 2} - 1 \right) \right\rfloor, \qquad (8)$$

where $I_{\rm src} = 1, 2, \ldots, F_{\rm src}$–1. In both cases, $I_{\rm reg}$ is defined to be $F_{\rm reg}$ when $I_{\rm src} = F_{\rm src}$. In practice, the quadratic matching rule (7) generally produces better results than the logistic rule (8) and it is the rule used in our numerical experiments.

III. Numerical results

We apply the Killing energy minimizing registration algorithm for cell images of live C2C12 cells obtained from experiments performed at the Genomic Laboratory, McGill University. They are nuclear tagged cell images. The frame rate is 7 to 10 minutes. Due to limited space, we only demonstrate a few examples here to illustrate how the registration method works. All computation is performed on a PC using MATLAB. The original image size is 512×512, but for illustration purpose, only the part of the image containing the cells of interest is shown whose size is around 100×100.

An image dataset with all the cells visible is taken as the ground truth. We then manually remove a cell from 8 frames to simulate the effect of a cell disappeared and reappeared in the image sequence. Note that the number of frames is for illustration purpose. The actual number of frames that a cell disappears may be different. The reconstruction results for the "missing" cell are shown in Fig. 2. In the original image frames, the cell moves gradually from the bottom part of the image to the middle right part with a slight change in size and appearance. The image results given by the Killing energy minimizing method generally agree well with the disappeared cell. It captures the translation motion correctly due to the effect of the Killing energy. Meanwhile, it also captures the cell expansion by the nonrigid particle part of the model. Furthermore, the cell appearance shows nice resemblance of the intensity variation inside the disappeared cell. In contrast, the particle nonrigid registration model alone generates unnatural motion, shape, and appearance of the disappeared cell. Fig. 3 shows another example where a cell have a rotational movement.

We then demonstrate the effect of gap size on the reconstruction given by the Killing minimizing registration method. In this case, we manually remove cells from 4, 8,

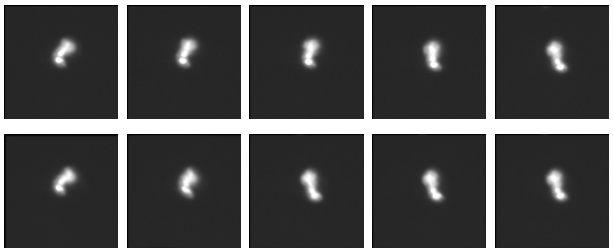

Fig. 3. (Top) original images, (bottom) reconstruction results of a cell with a rotational movement given by the Killing energy minimizing registration.

and 12 frames. The reconstruction results for the "missing" image frames are shown in Fig. 4. The registration results in general agree with the ground truth very well, with better results for smaller gap sizes and tend to get worse when the gap size increases. This illustrates a limitation of the model when the template and target images are vastly different, which is also common to many registration methods.

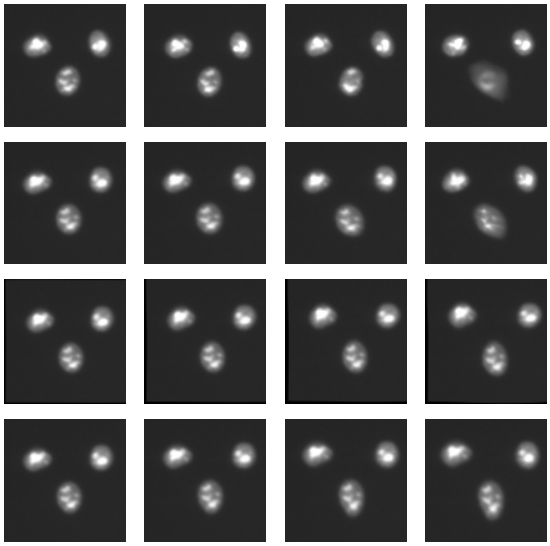

Fig. 4. (Row 1) original images. (Row 2)-(Row 4) reconstruction results of image frames where cells are removed from a gap of size 4 frames, 8 frames, and 12 frames, given by the Killing energy minimizing registration. Only the first 4 reconstruction images are shown.

In another experiment, we compute the error of the registration reconstruction for cells disappeared for 8 frames. Ten datasets are tested with a total of 80 image registration results. Error is measured as the mean squared difference between the reconstruction images and the ground truth. The results are given in Fig. 5. The error is around 10^{-3} near the ends and increases slightly in the middle.

Finally, we show the reconstruction results for the case of a cell division; see Fig. 6. The Killing energy minimizing registration model is able to reproduce the splitting of the missing cell.

IV. Conclusion

We have presented a novel registration model for reconstructing incomplete cell paths for tracking cells in fluorescent images when some of the cells become invisible

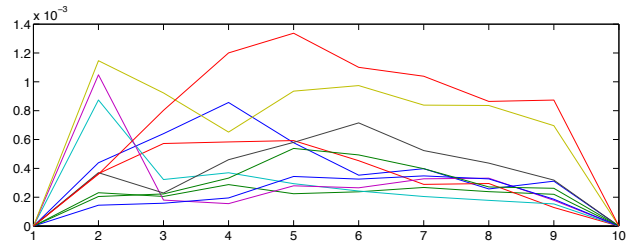

Fig. 5. Error of reconstruction results given by the Killing energy minimizing registration for 10 testing cases, each with a gap of 8 frames.

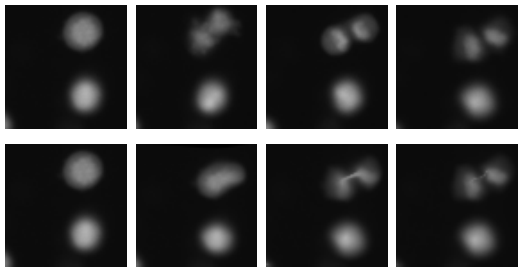

Fig. 6. (Top) Four image frames in which a cell was proceeding through a cell division were replaced by blank image frames to simulate the disappearance of the cell, (bottom) reconstruction of the four missing frames given by the Killing energy minimizing registration model.

in the image sequence. By aligning the images before and after the cell disappeared by a particle nonrigid registration model, together with the technique of enforcing KVF into the model, we have shown that our Killing energy minimizing registration model is able to reconstruct missing cells with natural movements and appearance. This is important to reliable cell tracking. We have demonstrated the effectiveness of the model by a number of examples from different live cell images.

References

[1] G. Rabut and J. Ellenberg, "Automatic real-time three-dimensional cell tracking by fluorescence microscopy," *Journal of Microscopy*, vol. 216, pp. 131–137, 2004.

[2] O. Dzyubachyk, W. van Cappellen, J. Esser, W. Niessen, and E. Meijering, "Advanced level-set-based cell tracking in time-lapse fluorescence microscopy," *IEEE Transactions on Medical Imaging*, vol. 29, pp. 852–867, 2010.

[3] M. Hariri and J. W. Wan, "Reconstruction of incomplete cell paths through a 3D-2D level set segmentation," in *Proceedings of SPIE Symposium on Medical Imaging: Image Processing, San Diego*, February 2012.

[4] A. Bosnjak, G. Montilla, R. Villegas, and I. Jara, "3D segmentation with an application of level set method using MRI volumes for image guided surgery," in *Proceedings of 29th Annual International Conference of the IEEE EMBS, Lyon, France*, August 2007, pp. 5263–5266.

[5] N. Leung and J. W. Wan, "Reconstruction of missing cells in fluorescent microscopy," in *Proceedings of 34th Annual International Conference of the IEEE EMBS, San Diego, USA*, August 2012, pp. 5323–5326.

[6] Z. Yi and J. W. Wan, "An inviscid model for nonrigid image registration," *Journal of Inverse Problems and Imaging*, vol. 5, pp. 263–284, 2011.

[7] J. Modersitzki, *Numerical Methods for Image Registration*. Oxford: Oxford University Press, 2004.

[8] P. Petersen, *Riemannian Geometry*. New York, USA: Springer, 2010.

[9] J. Solomon, M. Ben-Chen, A. Butscher, and L. Guibas, "As-killing-as-possible vector fields for planar deformation," *Computer Graphics Forum*, vol. 30, no. 5, pp. 1543–1552, 2011.